Extended Self-Similarity in Turbulent Systems: An Analytically Soluble Example

Daniel Segel,* Victor L'vov,† and Itamar Procaccia‡
Department of Chemical Physics, The Weizmann Institute of Science, Rehovot 76100, Israel
(Received 6 November 1995)

In turbulent flows the nth order structure functions $S_n(R)$ scale like R^{ζ_n} when R is in the "inertial range." Extended self-similarity refers to the substantial increase in the range of power law behavior of the $S_n(R)$ when they are plotted as a function of $S_2(R)$ or $S_3(R)$. Here we demonstrate this phenomenon analytically in the context of the "multiscaling" turbulent advection of a passive scalar. This model gives rise to a series of differential equations for the structure functions $S_n(R)$ which can be solved and shown to exhibit extended self-similarity. The phenomenon is understood by comparing the equations for $S_n(R)$ to those for $S_n(S_2)$.

PACS numbers: 47.27.Gs, 05.40.+j, 47.27.Jv

The fundamental theory of turbulence concerns itself with the universality of the small scale structure of turbulent flows and its characterization by universal scaling laws [1]. Since the days of Kolmogorov [2], one expects the structure functions $S_n(R)$ to scale with R as long as R is the inertial range, i.e.,

$$S_n(R) \sim R^{\zeta_n}, \quad \text{for} \quad \eta \ll R \ll L. \tag{1}$$

Here η and L are the viscous and outer lengths, respectively. For a given turbulent field $u(\mathbf{r}, t)$ the nth order structure function is defined as $S_n(R) = \langle [u(\mathbf{r} + \mathbf{R}, t) - u(\mathbf{r}, t)]^n \rangle$ where the angular brackets $\langle \cdots \rangle$ denote an average over $\mathbf{r}$ and t. Kolmogorov's 1941 picture of turbulence (K41) predicted that the exponents of the structure functions of the velocity field satisfy $\zeta_n = n/3$. Further research along the same lines suggested that the structure functions of passive scalar densities also have the same exponents [3,4]. On the hand, experiments [5,6] have indicated deviations from this scaling and even the possibility of multiscaling, i.e., a nonlinear dependence of ζ_n on n. These findings raise fundamental questions as to our understanding of the universality of the small scale structure of turbulence.

Unfortunately, the experimental measurement of the scaling exponents in turbulent flows is hampered by the fact that the range of scales that exhibit scaling behavior is rather small for Reynolds numbers Re accessible to date. Even though the viscous scale η decreases like $\mathrm{Re}^{-3/4}$, the scaling behavior (1) is expected to set in only at about 10η, and cease at about $L/100$. Thus even at $\mathrm{Re} \sim 10^7$ the inertial range is not broad enough to allow accurate measurements of ζ_n, particularly for larger values of n.

A partial resolution of these difficulties has been recently offered [7] by changing the way that the experimental data are presented. Instead of plotting log-log plots of $S_n(R)$ vs R, it was argued that plotting log-log plots of $S_n(R)$ vs $S_2(R)$ or $S_3(R)$ reveals much longer scaling ranges that can be used to fit accurate exponents. This method was dubbed *extended self-similarity*. While the effectiveness of this method has been demonstrated [8], the reason for its success remains unclear. Therefore its reliability is not guaranteed. The aim of the Letter is to address this method theoretically for Kraichan's model of a passive scalar advected by a very rapidly varying velocity field [9]. In this model multiscaling is known to occur [10–12], and we have sufficient analytic understanding of the mechanism of (multi)scaling to assess why extended self-similarity could hold. One should stress that in the case of normal scaling extended self-similarity can be rationalized rather straightforwardly [13]. To our knowledge no analytic demonstration of this effect is available in a case exhibiting multiscaling.

In this model the equation for the passive scalar concentration $T(\mathrm{x})$ is given by

$$\frac{\partial T}{\partial t} + (\mathbf{u} \cdot \boldsymbol{\nabla}) T = \kappa \nabla^2 T, \tag{2}$$

where the velocity field $\mathbf{u}$ is taken as Gaussian random and with a δ-function correlation in time. The structure functions $S_{2n}(R)$ are known to obey the differential equations [9,11]

$$-R^{1-d} \frac{\partial}{\partial R} R^{d-1} h(R) \frac{\partial}{\partial R} S_{2n}(R) = J_{2n}(R). \tag{3}$$

Here $h(R) = H(R/\mathcal{L})^{\zeta_h}$ for $R < \mathcal{L}$, where H is a dimensional constant and $\mathcal{L}$ is some characteristic outer scale of the driving velocity field. The scaling exponent ζ_h is a chosen parameter in this model, taking any desired value in the interval (0,2). The function $J_{2n}(R)$ is known exactly for R in the inertial range [10,11], but for our purposes we need to know it also in the near viscous range. A form that is appropriate in both ranges has been suggested by Kraichnan [10]:

$$J_{2n}(R) = 2n\kappa \frac{S_{2n}(R)}{S_2(R)} [\nabla^2 S_2(R) - \nabla^2 S_2(0)]. \tag{4}$$

This form has been recently supported by numerical simulations [14]. In the inertial range the last two equations have a multiscaling solution for $S_{2n}(R)$ with the exponents

$$\zeta_{2n} = \frac{1}{2}\left[\sqrt{(3 - \zeta_2)^2 + 12n\zeta_2} + \zeta_2 - 3\right]. \tag{5}$$

 0031-9007/96/76(11)/1828(4)$10.00

Our first step in studying the issue of extended self-similarity using Eqs. (3) and (4) is to nondimensionalize them. Rescale lengths by $r_d \equiv \mathcal{L}(\kappa/H)^{1/\zeta_h}$ and the scalar density by $\Theta = r_d\sqrt{\epsilon/\kappa}$. The dimensionless functions $D_{2n}(y)$ are

$$D_{2n}(y) \equiv S_{2n}(yr_d)/\Theta^{2n}, \quad y \equiv R/r_d\,. \tag{6}$$

They satisfy the equations

$$\frac{d^2D_{2n}}{dy^2} + \frac{2+\zeta_h}{y}\frac{dD_{2n}}{dy} = \frac{2nD_{2n}}{y^{\zeta_h}D_2} \times \left[1 - \frac{1}{y^2}\frac{d}{dy}\left(y^2\frac{dD_2}{dy}\right)\right]. \tag{7}$$

The success of extended self similarity for this model can be assessed from Fig. 1, which compares plots of D_{2n} vs y with plots of D_{2n} vs D_2. The data are based on the numerical solution of Eq. (7) using IMSL/IDL's Adams-Gear ordinary differential equation (ODE) solver. The efficacy of extended self-similarity speaks for itself.

Next we exhibit the phenomenon analytically by finding the first order dissipative correction to the inertial range scaling of the structure functions. In the inertial range the exponent of $D_2(y)$ is $\zeta_2 = 2 - \zeta_h$ [9]. We can find the first correction to the power law, going into the dissipation range, by writing $D_2(y) = 2y^{\zeta_2}/3\zeta_2 + \epsilon(y)$. We then find the following ODE for $\epsilon(y)$:

$$\frac{d^2\epsilon}{d^2y} + \frac{2+\zeta_h}{y}\frac{d\epsilon}{dy} + \frac{4(3-\zeta_h)}{3y^{2\zeta_h}} = 0\,. \tag{8}$$

There are two possibilities for the leading order solution of this equation. If all the terms are of the same order the solution is $\epsilon_1 = -2y^{2-2\zeta_h}/3(1-\zeta_2)$. If the first two terms are larger we have $\epsilon_2 = B_2 + \epsilon_1$, where now ϵ_1 appears as the next order correction after a constant B_2. One can see that the dominant solution for small ζ_h is ϵ_1, with a transition to ϵ_2 at $\zeta_h = 1$. Thus the near-inertial solution for D_2 is

$$D_2(y) = \begin{cases} \dfrac{2y^{\zeta_2}}{3\zeta_2}\left(1 - \dfrac{\zeta_2 y^{\zeta_2-2}}{1-\zeta_2}\right) & \text{for } \zeta_h < 1\,, \quad (9) \\ \dfrac{2y^{\zeta_2}}{3\zeta_2}\left(1 + \dfrac{C_2}{y^{\zeta_2}}\right) & \text{for } \zeta_h > 1\,, \quad (10) \end{cases}$$

where C_2 is a constant. Note that for the case $\zeta_h = \frac{2}{3}$ the ODE for $D_2(y)$ can be solved exactly in terms of elementary operations, and the results are consistent with this solution.

Next we repeat this procedure for $D_{2n}(y)$. We substitute $D_{2n}(y) = A_{2n}y^{\zeta_{2n}}[1 + \xi(y)]$ in Eq. (7). For the case $\zeta_h > 1$ we find

$$\frac{d^2\xi}{dy^2} + \frac{1}{y}\frac{d\xi}{dy}(2\zeta_{2n} + 4 - \zeta_2) + \frac{3nC_2\zeta_2}{y^{2+\zeta_2}} = 0\,, \tag{11}$$

with a leading order scaling solution $\xi(y) = B_{2n}y^{-\zeta_2}$. The constant B_{2n} is found from Eq. (11) and the final result for $\zeta_2 < 1$ is

$$D_{2n}(y) = A_{2n}y^{\zeta_{2n}}\left[1 + \frac{3nC_2}{(2\zeta_{2n} + 3 - 2\zeta_2)y^{\zeta_2}}\right]. \tag{12}$$

At this point we can assess the efficacy of extended self-similarity (ESS) for the case $\zeta_h > 1$. If all functions D_{2n} were an exact power law in argument D_2 we would have

$$D_{2n}^{\mathrm{ESS}}(y) = [2(y^{\zeta_2} + C_2)/3\zeta_2]^{\zeta_{2n}/\zeta_2}, \tag{13}$$

or to the same order

$$D_{2n}^{\mathrm{ESS}}(y) = A_{2n}y^{\zeta_{2n}}(1 + \zeta_{2n}C_2/\zeta_2 y^{\zeta_2})\,. \tag{14}$$

The ratio r_1 between the coefficients of $y^{-\zeta_2}$ in Eqs. (12) and (14) measures the effectiveness of this presentation. Using Eq. (5) one finds

$$r_1 = \frac{3n\zeta_2}{\zeta_{2n}(2\zeta_{2n} + 3 - 2\zeta_2)} = \frac{n\zeta_2}{2n\zeta_2 - \zeta_{2n}}\,. \tag{15}$$

If $r_1 = 1$ we would have perfect extended self-similarity; $r_1 = 0$ is what we would get if we just plotted S_{2n} as a function of r. In Fig. 2(a) we can see a graph of r_1 as a function of ζ_2 for $n = 2, n = 4$, and $n = 6$. We can see that r is always in the interval $[\frac{1}{2}, 1]$: from Eq. (5) $\lim_{n\to\infty} r_1 = \frac{1}{2}$, and from Eqs. (5) and (15) $\lim_{\zeta_2\to 0} r_1 =$

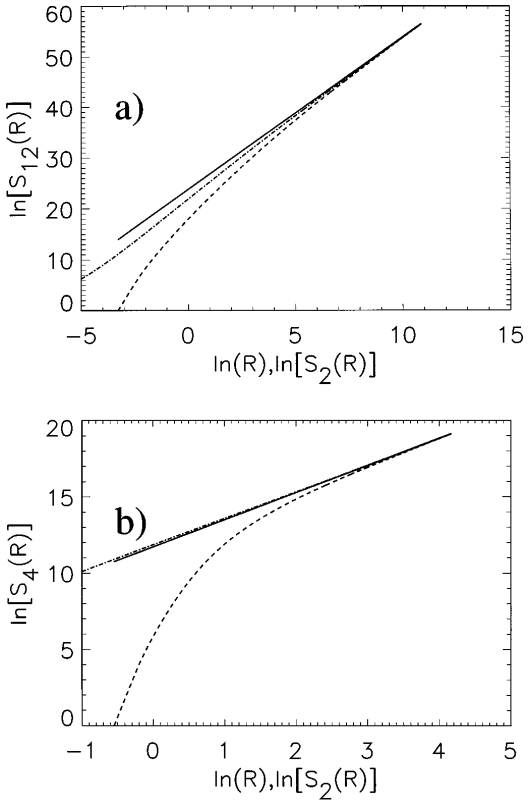

FIG. 1. The dimensionless structure functions $D_{2n}(y)$ plotted in ln-ln plots as functions of y (dashed line) and $D_2(y)$ (dash-dotted line), respectively. In the solid line the exact scaling law is shown. In panel (a) $\zeta_h = \frac{1}{2}$ and $n = 6$ and in panel (b) $\zeta_h = \frac{3}{2}$ and $n = 2$, good and bad examples of ESS in our model, respectively. One sees an improvement of the scaling law of at least 2 decades.

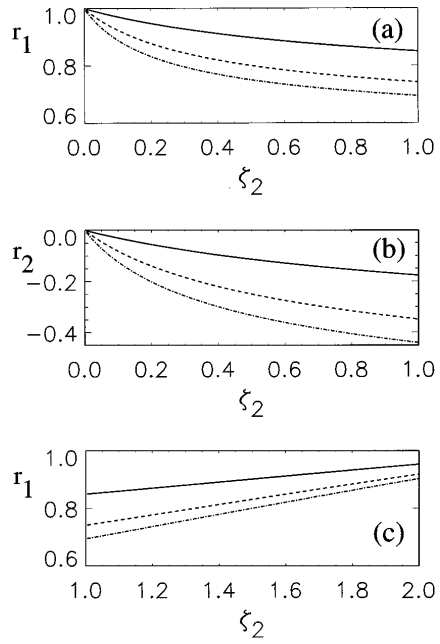

FIG. 2. (a) the ratio r_1 of Eq. (15) as a function of ζ_2 for $n = 2$ (solid line), $n = 4$ (dashed line), and $n = 6$ (dot-dashed line). (b) The ratio r_2 of Eq. (25) for the same values of n. (c) The ratio r_1 of Eq. (15) for $\zeta_2 > 1$, and the same values of n.

1. The convergence to $\frac{1}{2}$ is rather slow and not uniform in ζ_2.

The main point of the extended self-similarity is that S_2 (which is a function of R) is a "better" variable than the distance R itself when it comes to scaling behavior. Thus to complete our analysis we want to write ODE's for the D_{2n} as a sum of the inertial range terms plus a remainder term. Changing variables and writing the D_{2n} as a function of D_2, we expect to find that now the remainder term in the ODE's with respect to argument D_2, when evaluated in terms of the inertial range estimates, is smaller than when using r as a variable. To this aim we introduce a new set of functions $F_{2n}(x)$ of argument $x = D_2(y)$, defined by $F_{2n}(x) \equiv D_{2n}(y)$. Then Eqs. (7) gives for $F_{2n}(x)$ the following ODE:

$$\frac{d^2F_{2n}}{d^2x} + \frac{2}{2 + [f(x)]^{2-\zeta_2}}\left[\frac{dF_{2n}}{dx} - \frac{nF_{2n}(x)}{x}\right] \times \left[\left(\frac{df}{dx}\right)^2 + \frac{(2-\zeta_2)}{f(x)}\frac{df}{dx}\right] = 0, \quad (16)$$

where $f(x)$ is the inverse function of $D_2(y)$: $f(x) = y$ if $x = D_2(y)$. Now let us introduce a third set of dimensionless structure functions $G_{2n}(x)$ such that

$$G_{2n}(x) \equiv D_{2n}(y), \quad x \equiv 2y^{\zeta_2}/3\zeta_2 . \quad (17)$$

Note that the functions F_{2n} and G_{2n} are identical in the inertial range, since one is a function of D_2 and the other is a function of its power law in the inertial range. Indeed, it will be seen below that they satisfy the same ODE in the inertial range with a power law solution x^{ζ_{2n}/ζ_2}. Using (7) one derives the following ODE for $G_{2n}(x)$:

$$\frac{d^2G_{2n}}{dx^2} + \frac{3}{\zeta_2 x}\left[\frac{dG_{2n}}{dx} - \frac{nG_{2n}(x)}{g(x)}\right] + \frac{3nG_{2n}(x)}{g(x)} \times \left(\frac{2}{3\zeta_2 x}\right)^{2/\zeta_2}\left[(\zeta_2 + 1)\frac{dg}{dx} + \zeta_2 x\frac{d^2g}{dx^2}\right] = 0, \quad (18)$$

with the function $g(x)$ satisfying $g(x) = D_2(y)$.

Consider first the $\zeta_2 < 1$ case, and use the near-inertial approximation for $D_2(y)$, Eq. (10). Inverting this relation we find the relevant approximation for f in terms of x, i.e.,

$$f(x) = (3\zeta_2 x/2)^{1/\zeta_2}(1 - 2C_2/3\zeta_2^2 x). \quad (19)$$

Using this and introducing constants C_{2n}^0, $D_{2n} = C_{2n}^0 \times x^{\zeta_{2n}/\zeta_2}$ in the remainder term we find that the near-inertial version of Eq. (16) is

$$\frac{d^2F_{2n}}{d^2x} + \frac{3}{\zeta_2 x}\left[\frac{dF_{2n}}{dx} - \frac{nF_{2n}(x)}{x}\right] + \frac{2C_2C_{2n}^0}{\zeta_2^3}(\zeta_{2n} - n\zeta_2)x^{\zeta_{2n}/\zeta_2 - 3} = 0. \quad (20)$$

Doing the same to Eq. (18) we have

$$\frac{d^2G_{2n}}{d^2x} + \frac{3}{\zeta_2 x}\left[\frac{dG_{2n}}{dx} - \frac{nG_{2n}(x)}{x}\right] + \frac{2C_2C_{2n}^0}{\zeta_2^2} nx^{\zeta_{2n}/\zeta_2 - 3} = 0. \quad (21)$$

Indeed, we see that the first lines of these equations, which are the inertial range contribution, are the same. Also the second lines are of the same order in y, but the ratio r_2 between the coefficients in these lines (the remainder terms) is

$$r_2 = (\zeta_{2n} - n\zeta_2)/n\zeta_2 . \quad (22)$$

Since the Hölder inequalities imply that $\zeta_{2n} \le n\zeta_2$, we have $|r_2| \le 1$; this means that indeed the remainder term that "spoils" the inertial range scaling to first order is smaller in the new representation. One can see, by solving Eq. (16) in terms of the coefficient of the remainder term, using $F_{2n}(x)$ to express $D_{2n}(y)$ and comparing with Eq. (12), that one should have the relation

$$r_2 = 1 - 1/r_1 . \quad (23)$$

Now comparing Eqs. (15) and (22) one sees that this relation is true. Extended self-similarity as represented by r_1 very near unity indeed translates into very small r_2, that is into a small remainder term. In Fig. 2(b) we can see r_2 as a function of ζ_2 for $n = 2$, $n = 4$, and $n = 6$. As $n \to \infty$ the ratio becomes poor, $r_2 \to -1$, but the convergence is slow as we can see from Fig. 2(b) and again not uniform in ζ_2, since one can verify that $\lim_{\zeta_2 \to 0} r_2 = 0$.

The situation for $\zeta_2 > 1$ is much messier algebraically although just the same procedure can be followed in principle. We have already given in Eq. (10) the near inertial form for $D_2(y)$ for $\zeta_2 > 1$; we now substitute

this and $D_{2n}(y) = A_{2n} y^{\zeta_{2n}}[1 + \xi(y)]$ [considered as a definition of $\xi(y)$] into Eq. (7) to find the equation

$$\frac{d^2\xi}{dy^2} + (2\zeta_{2n} + 4 - \zeta_2)\frac{1}{y}\frac{d\xi}{dy} + \frac{n\zeta_2(1 + 2\zeta_2)(2 - \zeta_2)}{(\zeta_2 + 1)} y^{\zeta_2 - 4} = 0. \quad (24)$$

This equation has a power law solution which leads to

$$D_{2n}(y) = A_{2n} y^{\zeta_{2n}}\left[1 + \frac{n\zeta_2(1 + 2\zeta_2)}{(1 - \zeta_2)(1 + 2\zeta_{2n})} y^{\zeta_2 - 2}\right] \quad (25)$$

(for $\zeta_2 > 1$), which gives

$$r_1 = n\zeta_2(1 + 2\zeta_2)/\zeta_{2n}(1 + 2\zeta_{2n}). \quad (26)$$

In Fig. 2(c) we can see r_1 as a function of ζ_2 for $n = 2$, $n = 4$, and $n = 6$. For very large n we can see that

$$\lim_{n\to\infty} r_1 = (1 + 2_2)/6 \in [\tfrac{1}{2}, \tfrac{5}{6}], \quad (27)$$

but the convergence is slow as we can see from Fig. 2(c) and again not uniform in ζ_2, since one can verify that $\lim_{\zeta_2\to 0} r_1 = 1$. Again one can verify that the efficacy of ESS is reflected in a smaller remainder term in the ODE for S_{2n} using S_2 as a variable, as expressed by a ratio r_2 for which here too $r_2 = 1 - r_1^{-1}$.

The success of the method in this case cannot be glibly extended to any turbulent system. We see from the analysis that the improvement in the scaling behavior of S_n when presented as a function of S_2 is *not* a fundamental result but a statement on the similar behavior of the structure functions going into the dissipation range. This is measured by the value of the parameter r_1 of Eq. (15). We can imagine in principle—although no examples are known—a system for which the dissipative scale for S_n is *smaller* than that for S_2. In such a system the method will not improve the scaling plots. In this passive scalar model the dissipative scales of all the structure functions are of the same order, as has been shown in [12]. This is one of the deep reasons for the success of the method in the present case. It is tempting to conjecture that the success of the method in Navier-Stokes turbulence is an indication that the dissipative scales of S_n are either of the same order or become larger with n. The full understanding of the method in that case must await a better analytic understanding of the structure functions and their functional form in the near dissipative regime.

*Electronic address: daniel@dvir.weizmann.ac.il
†Electronic address: fnlvov@wis.weizmann.ac.il
‡Electronic address: cfprocac@weizmann.weizmann.ac.il

[1] For a recent text, see Uriel Frisch, *Turbulence: The Legacy of A. N. Kolmogorov* (Cambridge University Press, Cambridge, 1995).
[2] A. N. Kolmogorov, Dokl. Akad Nauk SSSR **30**, 229 (1941).
[3] A. M. Obukhov, Izv. Akad. Nauk SSR ser., Geogr. Geofiz. **13**, 58 (1949).
[4] S. Corrsin, J. Appl. Phys. **22**, 469 (1949).
[5] F. Anselmet, Y. Gagne, E. J. Hopfinger, and R. A. Antonia, J. Fluid Mech. **140**, 63 (1984).
[6] C. Meneveau and K. R. Sreenivasan, Nucl. Phys. B, Proc. Suppl. **2**, 49 (1987).
[7] R. Benzi, S. Ciliberto, R. Tripiccione, C. Baudet, F. Massaioli, and S. Succi, Phys. Rev. E **48**, R29 (1993).
[8] R. Benzi, S. Ciliberto, C. Baudet, G. Ruiz Chavarria, and R. Tripiccione, Europhys. Lett. **24**, 275 (1993).
[9] R. H. Kraichnan, Phys. Fluids **11**, 945 (1968).
[10] R. H. Kraichnan, Phys. Rev. Lett. **72**, 1016 (1994).
[11] A. L. Fairhall, O. Gat, V. S. L'vov, and I. Procaccia, Phys. Rev. E (to be published).
[12] V. L. L'vov and I. Procaccia, "Fusion Rules in Turbulent Systems with Flux Equilibrium" (to be published).
[13] V. S. L'vov and I. Procaccia, Phys. Rev. E **49**, 4044 (1994).
[14] R. H. Kraichnan (private communication).